Astroparticle Physics 67 (2015) 1–7

Contents lists available at ScienceDirect

Astroparticle Physics

journal homepage: www.elsevier.com/locate/astropart

Yearlong moored bioluminescence and current data at KM3NeT neutrino telescope sites in the deep Ionian Sea

Hans van Haren [a,*], Maarten de Jong [b,c], Paul Kooijman [b,d]

[a] NIOZ Royal Netherlands Institute for Sea Research, P.O. Box 59, 1790 AB Den Burg, The Netherlands
[b] Nikhef, Science Park 105, 1098 XG Amsterdam, The Netherlands
[c] Leids Instituut voor Onderzoek in Natuurkunde, Universiteit Leiden, 2333 CA Leiden, The Netherlands
[d] Instituut Hoge-Energie Fysica, Universiteit van Amsterdam, Science Park 105, 1098 XG Amsterdam, The Netherlands

ARTICLE INFO

Article history:
Received 4 June 2014
Received in revised form 7 January 2015
Accepted 26 January 2015
Available online 31 January 2015

Keywords:
Neutrino telescope site
Stand-alone optical sensors
Correlation of bioluminescence with current
Opposing phases for opposing optical sensors

ABSTRACT

Yearlong observations are presented using stand-alone small optical sensors and current meters in the deep Ionian Sea, E-Mediterranean. At two future neutrino telescope sites, off Sicily (I) and off Peloponessos (Gr), we deployed 2500–3000 m long mooring lines with oceanographic instrumentation. At about 150 m above the sea-floor, a glass sphere was mounted to each line holding two 3″-diameter photo-multiplier-tubes 'PMTs' in opposing directions for a first deep-sea test. Due to technical problems the background optical count rate could not be well established. Here, the focus is on the variations with time of bioluminescence bursts and their correlation with currents. Spectral analysis demonstrates that the PMT data best resemble those of horizontal currents (kinetic energy), significantly peaking at near-inertial, sub-inertial mesoscale and (Gr only) at tidal frequencies. Out-of-phase differences between signals from opposing PMTs in the same optical unit indicate impacts of bioluminescent organisms as a function of current direction, rather than a bacterial glow constant with time.

1. Introduction

The optical properties of seawater are important for ocean life as many animals rely for their food-supply on vision, whether supported by ambient solar light in the upper few 100 m near the surface, or by activated light-source known as 'bioluminescence'. Such activation can be invoked by the animal (or in some cases, plant) itself, but quite often also through an exterior impulse, e.g., when the animal is hit by an object.

Likewise, optical properties of seawater are important for astrophysical researchers who use the deep-sea as a medium for an underwater neutrino telescope. For them, bioluminescence can be a nuisance, as activation often occurs upon impact, for example with a telescope, e.g., [1]. It is thus important to know what the bioluminescent part of the optical properties of water are at a given neutrino telescope location, and what the probable light source (intensities) locally can be. Therefore, one could lower an optical package from a ship to obtain vertical profiles of such properties [1–4]. Alternatively, one could deploy a mooring array holding sensors to obtain a time series of optical properties at a given depth. This is done at neutrino telescope site ANTARES [5] off Toulon (F) using a cabled network, but only over brief periods of time near future telescope sites off Sicily (I) and off Peloponessos (Gr).

The three deep Mediterranean sites constitute 'KM3NeT', a European deep-sea research infrastructure, that will host a network of neutrino telescopes with a volume of several cubic kilometers [6]. The telescope will be used to search for neutrinos from distant astrophysical sources like gamma ray bursters, supernovae or colliding stars and will be a powerful tool in the search for dark matter in the Universe. These sites are in the Northern Hemisphere, to complement the IceCube-telescope in Antarctica, and in the Mediterranean Sea where sufficiently deep waters are found within several tens of kilometers from coasts.

Here, we present yearlong observations using moored test-optical and current stand-alone sensors from the Ionian Sea (E-Mediterranean). The test-deployments include the use of relatively small, 3″-diameter experimental photo multip1ier tubes (PMT) as optical sensors at great depths. Similar small PMTs will also be used in future KM3NeT assemblies [7,8], although probably of different make like Hamamatsu R12199-02 and ETEL D783FL PMTs presently tested [9]. Our analysis focuses on the relative variability of optical properties with time, due to bioluminescence, and on the level of coherency with current variations in particular frequency

* Corresponding author.
E-mail address: hans.van.haren@nioz.nl (H. van Haren).

http://dx.doi.org/10.1016/j.astropartphys.2015.01.005
0927-6505/

bands. The precise background levels posed a problem for the present experimental PMTs but are irrelevant for our analysis.

2. Data

In December 2009, two 2500–3000 m long deep-sea moorings were deployed near two future neutrino telescope sites in the Ionian Sea: at 100 km East of Capo Passero (CP), Italy, and at 40 km West of Pylos (Py), Greece. Thirteen months later they were recovered. See Table 1 for mooring details. The moorings were 28 km NNW and 11 km NW from the proposed future KM3NeT-sites, respectively. The lines had 300–350 kg net buoyancy. They held a number of stand-alone, internally recording, oceanographic instruments, including current meters, pressure sensors and, in the lower 300 m above the bottom (mab) high-resolution temperature sensors. The latter sensors revealed deep-sea motions dominated by inertial currents, governed by the rotation of the Earth, and which resulted in very large (>150 m) amplitude internal waves and associated turbulent convection in the weakly density-stratified waters [10].

In each mooring, about 150 m above the bottom, a test Optical Module (OM) built at Nikhef was mounted to the cable. The OM (Fig. 1) consisted of two 3″-diameter Photonis XP53B20 PMTs (see for their technical performance, e.g., [7,8]) that were packed with data-storage-electronics and batteries inside a 17″-diameter glass sphere. For overboard handling, the glass spheres were held in protective plastic caps, with openings cut-out for the PMTs. The PMTs were operated with a gain of 1×10^6. During consecutive periods of 2160 s (36 min), all PMT signals above an equivalent threshold of 0.3 photo-electrons were counted. The corresponding PMT count rates (PCR) were measured with a dynamic range of 0–40 kHz and logged for the entire deployment period. The sensitive areas of the PMTs were oriented back-to-back at an angle of 45 degrees below the horizon to avoid a possible degradation due to biofouling. For this stand-alone deep-sea test of the particular 3″-PMTs, the electronics were as simple as possible. Unfortunately, no compass was mounted with these sensors. However, the OM was expected to orient with the current, in the same fashion as the nearby current meter that did provide compass readings.

Just 5 m above each OM, a Nortek AquaDopp acoustic current meter was attached to the line, with additional compass, pressure and tilt sensors. These instruments sampled once every 900 s.

3. Observations

Of the four PMTs, three (one near CP: CP-a, two near Pylos: Py-a, Py-b) delivered useful time series of 36-min average PCR (Fig. 2). The optical backgrounds observed in the deep sea comprise two contributions; a continuous component from radioactive decays of Potassium (and possibly bacteria) plus a bursting component due to macroscopic organisms. The Potassium concentration in the sea is essentially constant and independent of the location. The biological light emission, however, can vary in time and location. The intensity and variability are not well understood. Specifically, the different decrease of observed PCR in the first 50 days at both sites is still unknown. The expected rate due to Potassium decays was calculated beforehand for a standard Bialkali photocathode and estimated to be 5 kHz with an uncertainty of 10%. The actual photo-cathode was composed of so-called super Bialkali yielding a higher quantum efficiency (QE). At that time, this photocathode material should be considered experimental and different PMTs showed different behavior. The dark counts of these PMTs are in general much higher, up to a factor of 5, than PMTs with standard Bialkali and strongly depend on the temperature and to some extent on the history of the PMT. The dark counts were measured beforehand and found to vary between 4 kHz and 50 kHz, depending on the temperature (typically 16–22 °C), elapsed time (8–48 h) and other parameters (such as environmental conditions) which could not be unambiguously defined. So, the dark counts could compromise the background PCR measurements. However, the conditions in the deep-sea are extremely stable and temperature did not vary by more than ±0.01 °C [10]. The available data were therefore analyzed based on the following two assumptions:

1. The expected PCR due to potassium decays ranges between 6 and 9 kHz.
2. The difference between the baseline of the observed PCR and the expected PCR due to potassium decays is simply attributed to the dark count of the PMT.

The assumed range of the expected PCR due to potassium decays covers an uncertainty of the QE of super Bialkali in the range of 1.2–1.8 times that of standard Bialkali. This range covers all values of the observed QEs of the PMTs. The second assumption implies that the PCR due to potassium decays cannot be unambiguously measured in situ due to the unknown dark count of the PMTs in situ. In the following, the ratio between the observed PCR and the baseline PCR is referred to as "normalized rate". The results of two data sets are presented in Fig. 3. (After the present measurements, new 3″-diameter PMTs have been developed using standard Bialkali. These new PMTs combine a (relatively) high QE with lowerdark counts and will be used for the KM3NeT neutrino telescope. The specifications of the new PMTs are presented in [6] and results from their first use showing background levels of 8–9.5 kHz at the Toulon-site are given in [9]). As we will perform spectral analysis, of signals varying relative to the background, we could have presented Fig. 2 without the, here irrelevant, arbitrary background levels. In comparison with the Toulon-site, where single hits caused 3″-PMT levels to exceed their background levels by about 20–25 kHz or by a factor of 2–3, the present data show increases above background by about half (CP) and by a third (Py) of those values, respectively.

The sporadic increases as a function of time of the normalized rate is used to identify possible harmonic signals in the PCR. These signals are best studied using Fourier-transform from the time- to the frequency (σ)-domain, and which by nature is sensitive to harmonic functions that may have a small amplitude in the time-domain [11]. Below, the Fourier-spectra are calculated using 29 half-overlapping 'Kaiser'-windows, slightly modified cosine-'Hanning' windows. This 'moderate' smoothing provides about 50 degrees of freedom.

The basic information gained from the time-domain-analysis incorporates the larger variability near CP and the considerable difference between the two sensors near Pylos. When zoomed, the latter two show a dominant semidiurnal tidal variability and, remarkable, a 180° phase difference, as will be clear from the spectral analysis in Section 3.2.

Table 1
Yearlong optical sensor – current meter mooring details from potential neutrino telescope sites in the Ionian Sea, E-Mediterranean. (mab = m above the bottom).

Mooring	Near Pylos (Gr)	Near Capo Passero (I)
Latitude	36°37.657′N	36°29.555′N
Longitude	21°24.907′E	15°54.826′E
Water depth	4450 m	3320 m
Deployment	15/12/09	18/12/09
Recovery	30/01/11	25/01/11
Optical sensors	Nikhef, 2160 s, 170 mab	Nikhef, 2160 s, 145 mab
Current meters	Nortek AquaDopp, 900 s, 175 mab	Nortek AquaDopp, 900 s, 150 mab

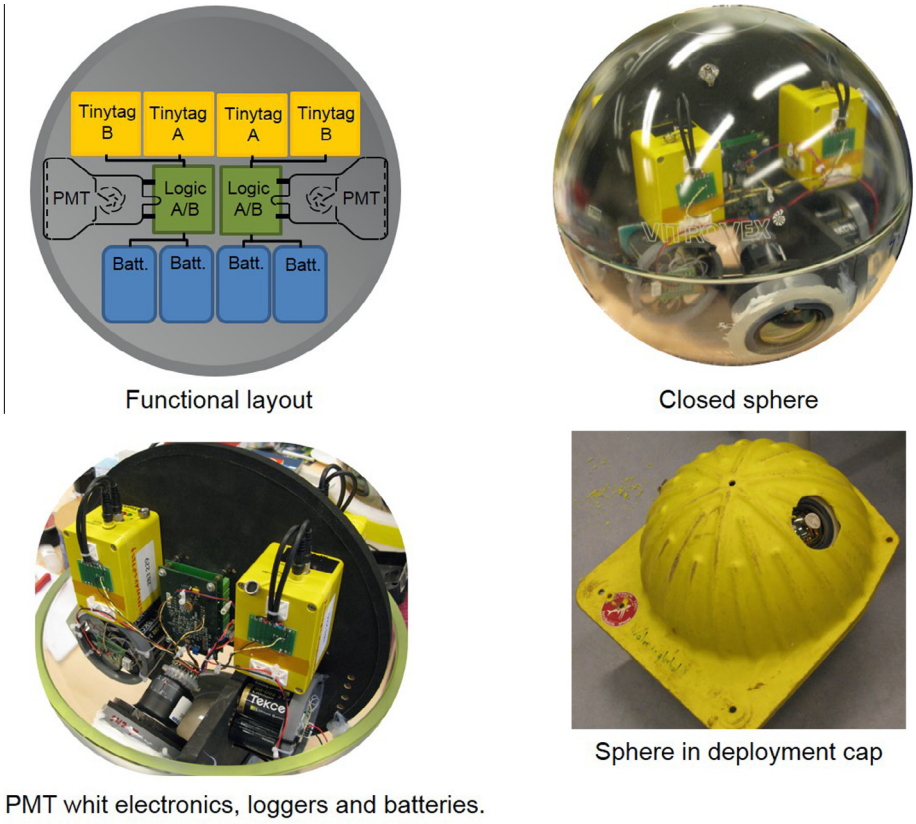

Fig. 1. Lay-out, electronics and mounting of in-situ recording PMT inside a glass sphere (OM).

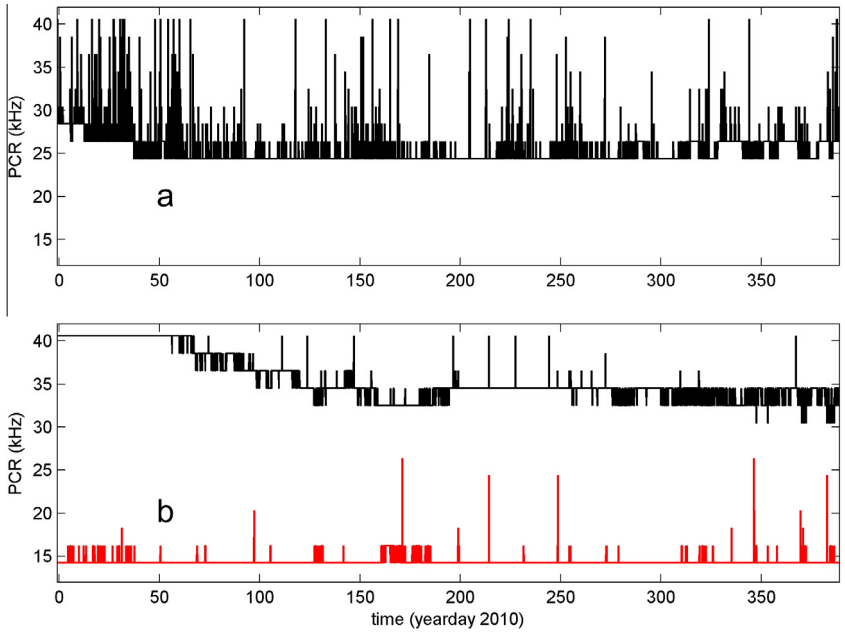

Fig. 2. Time series, at original 36 min intervals, of yearlong moored average optical count rates (PCR) in the Ionian Sea. (a) A single sensor CP-a from about 3200 m at a site near Capo Passero, Italy. (b) Two, sensor Py-a (black) and sensor Py-b (red), from about 4300 m at a site near Pylos, Greece. (For interpretation of the references to color in this figure legend, the reader is referred to the web version of this article.)

These optical records were little affected by undesirable mooring motions due to current drag. The long moorings were designed for minimal drag by currents using sufficiently large buoyancy. The pressure and tilt sensor records demonstrated that artificial mooring motions were below noise level (~0.1 dBar for the pressure sensor near CP). This was confirmed by the dominant periodic variations in both pressure and current records, which are tidal (semidiurnal and diurnal) for pressure and inertial (due to the rotation of the Earth) for currents (see also Figs. 4 and 6 below). This implies that current drag does not dominate pressure variations, as inertial and tidal bands are well-separated in frequency.

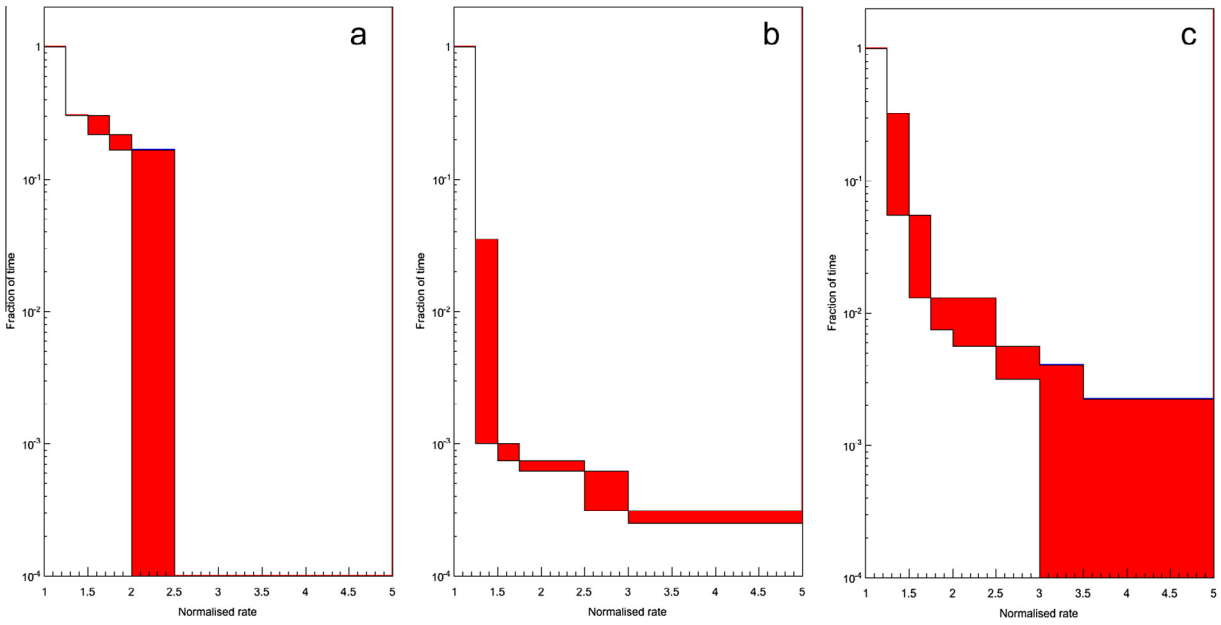

Fig. 3. Fraction of the time that the observed rate is a factor higher than the calculated rate due to Potassium decays and the PMT dark count. (a) Near Pylos (Py-a). (b) Near Pylos (Py-b). (c) Near Capo Passero. The red areas correspond to the uncertainty on the QE of the PMTs (see text). (For interpretation of the references to color in this figure legend, the reader is referred to the web version of this article.)

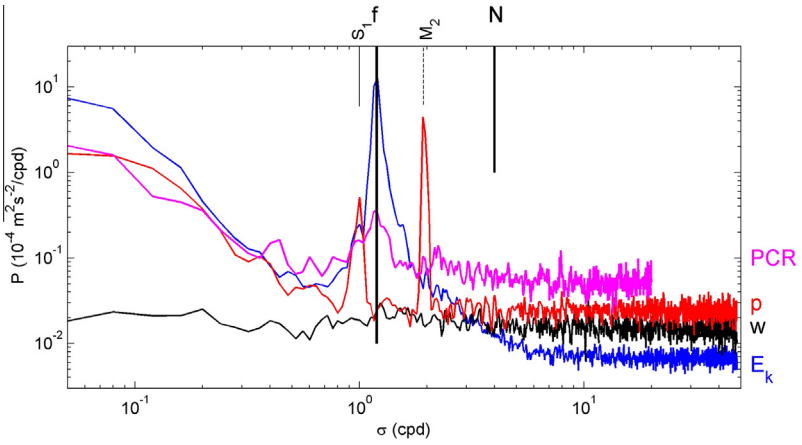

Fig. 4. Spectra of yearlong moored observations from 3200 m near CP. Average optical count rates (purple; PCR; CP-a) are compared with nearby observed pressure (red; p), vertical velocity (black; w) and kinetic energy (blue; E_k). The vertical scale is for E_k, w; the two others are arbitrarily offset vertically. Denoted frequencies: S_1 = diurnal solar tidal, f = inertial, M_2 = semidiurnal lunar tidal, N = buoyancy. (For interpretation of the references to color in this figure legend, the reader is referred to the web version of this article.)

3.1. Spectral analysis of observations near CP

The pressure sensor records were dominated by the hydrostatic barotropic ('surface') semidiurnal tide of 0.05–0.1 dBar (0.1 dBar is about 1 m in vertical displacement) amplitude, a weaker diurnal tide and by sub-inertial mesoscale ($0.05 < \sigma < 0.2$ cpd, cycle per day; 5–20 day periodic) variations of similar amplitude. This results in three major 'peaks', in its spectrum (Fig. 4, red). The horizontal currents are dominated by inertial and mesoscale motions, with relatively weak semidiurnal tides (Fig. 4). Horizontal current components [u, v], for [East–West, North–South], contribute most to the total kinetic energy $E_k = (u^2 + v^2 + w^2)$, as vertical current component $w \ll u, v$ in general. A small and broad peak is visible in the w-spectrum around the inertial frequency f (Fig. 4, black).

The PCR-spectrum shows large variance at sub-inertial mesoscales and around f (Fig. 4, purple). This suggests a partial correspondence between (horizontal) currents and optical data. Weak, but significant coherence is found at these frequencies between PCR and horizontal current components (Fig. 5(a)), suggesting larger optical activity associated with variations in amplitude and direction of advecting currents, or in the current-components. No significant coherence is found between PCR and the current magnitude only, which implies no evidence of the effect on optical data by larger impact (due to collisions with the glass spheres containing the PCR-sensors).

Coherent phase differences (Fig. 5(b)) between east current component u, also representative of north component v, and PCR are typically around 180° for sub-inertial mesoscale motions and around 0°, 360° for inertial motions. (It is noted that when the coherence is below the 95% significance level, indicated by the dashed horizontal line in panel a, the phase is scattered over all directions between neighboring frequency bands. See for example

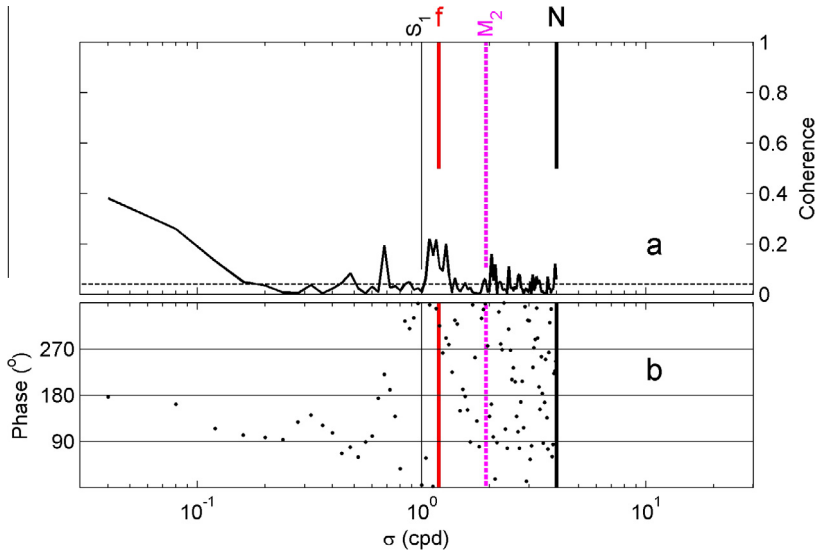

Fig. 5. Correlation between PCR-data from CP-a and nearby east(u)-current component. (a) Coherence, the horizontal dashed line indicates the 95% statistical significance level. (b) phase.

around σ = N, the buoyancy frequency indicating the highest internal wave frequency). The inertial motions show a broader band for coherence (Fig. 5(a)) than for the peak in power but which is similar in width to the base in power (Fig. 4).

3.2. Spectral analysis of observations near Pylos

Near Pylos the pressure spectrum (Fig. 6, red) is dominated by three peaks, at the diurnal and semidiurnal tidal frequencies, and, because of the reduced pressure-sensor noise, at the terdiurnal interaction frequency. All frequency bands are relatively narrow, thus representing highly deterministic signals, dominated by the surface elevation, mainly. Besides the familiar broader peaked near-inertial band dominating the kinetic energy spectrum, some moderate peak is observed at the semidiurnal tidal frequencies (Fig. 6, blue). The vertical current is also broad and weakly peaking at f (Fig. 6, black). This broad band is seen to roll-off to the horizontal white noise level approximately at the mean buoyancy frequency. This is partially coincidental, because of the noise level, but very typical for the deep Mediterranean. It has also been observed in the deep occidental basin [12].

Besides a relatively large variance at sub-inertial mesoscales and around f, the Py-a PCR-spectrum (Fig. 6, purple) shows peaks at tidal frequencies. This suggests a direct correspondence between PCR and currents, but also with the hydrostatic surface pressure variations, even though the former are small fluctuations $O(10^3)$ N m^{-2} around mean static pressure of about 4×10^7 N m^{-2}.

The tidal coherence is particularly large and narrow-peaked between u and Py-a PCR (Fig. 7), but especially also between p and PCR (not shown). The tidal phase difference, whilst broadly around 270° for u and PCR from Py-a, is about 90° between u and PCR from Py-b (not shown). The out-of-phase relationship between the two PMT-sensors near Pylos is quantified in Fig. 8; at frequencies at which coherence is found significant (above the dashed line in Fig. 8(a)), the phase difference near 180° clearly dominates. As the two PMTs were mounted on different sides of the OM, *cf.* Fig. 1, this 180°-out-of-phase relationship either reflects the changes in current direction (for an OM fixed in space), or an OM rotating around its swivel more or less in phase with the current so that one PMT is oriented on the impact side and the other not. Although the OM lacked a compass, the nearby current meter compass showed continual orientation with the current. In both cases, this indicates the variation with time in optical output is due to the impact of bioluminescent organisms, and not to a 'quasi-constant' bacterial glow. It is noted that the spectral form (not shown) of Py-b time series (Fig. 2(b) red) more resembles the PCR-spectrum near CP (Fig. 4).

4. Discussion: comparing the two sites

Major differences between the two sites are the current amplitudes, which are found nearly two times larger near CP (Fig. 4; maximum current speed $|U|_{max} = 0.14$ m s^{-1} at 400 mab, m above the bottom), compared with near Pylos (Fig. 6; identical scales as Fig. 4; $|U|_{max} = 0.08$ m s^{-1}). For the tidal currents however, they are a factor of two larger near Pylos than near CP.

The vertical current is better visible in the observations from near Pylos than from near CP. This suggests on average somewhat weaker local vertical density stratification in the deep-sea near Pylos. This is because near-inertial motions, which are purely horizontal in strong stratification, turn away from gravity towards the Earth rotational vector [13]. The aspect (variance) ratio $(|w|^2/|u|^2)|_f \approx 0.1$ as observed near Pylos, where in the well-stratified open ocean values of 10^{-4} or smaller are not uncommon at large scales. It implies that at the present mooring sites near f substantial mean vertical current amplitudes can be reached of $|w|_f \sim 0.01$ m s^{-1}, with $|u|_f \sim 0.03$ m s^{-1}. Such vertical currents generate vertical displacements of some 200 m, as their half-period is about 10 h, with considerable impact on the redistribution of small-scale life, notably zooplankton [10].

Although the PCR-spectra and time series seem to differ considerably between the sites, their correlation with horizontal velocity components is similar, both in coherence and phase (*cf.* Figs. 5 and 7), except for the semidiurnal peak for Py-a.

5. Conclusions

Following a spectral comparison of variations with time of poorly resolved optical sensor data with nearby current and hydrostatic pressure observations from the same moorings it is concluded that,

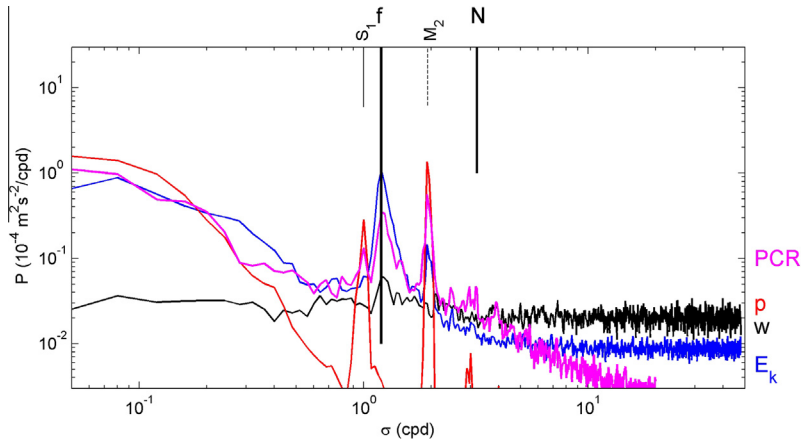

Fig. 6. As Fig. 4, but for PCR-sensor Py-a (black line in Fig. 2(b)). Note that the associated pressure sensor has a tenfold better s–n ratio than the one for Fig. 4. Likewise, the PCR-observations are less noisy than the ones in Fig. 4.

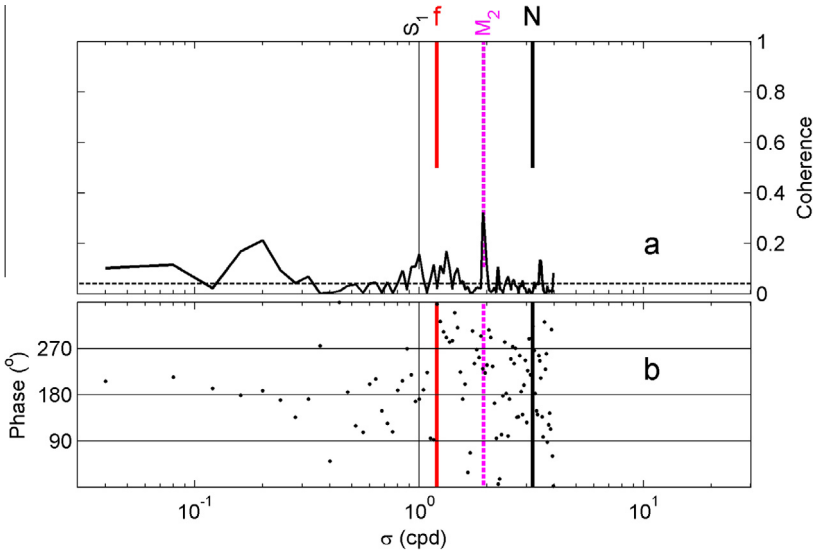

Fig. 7. As Fig. 6, but for sensor Py-a and its nearby current meter.

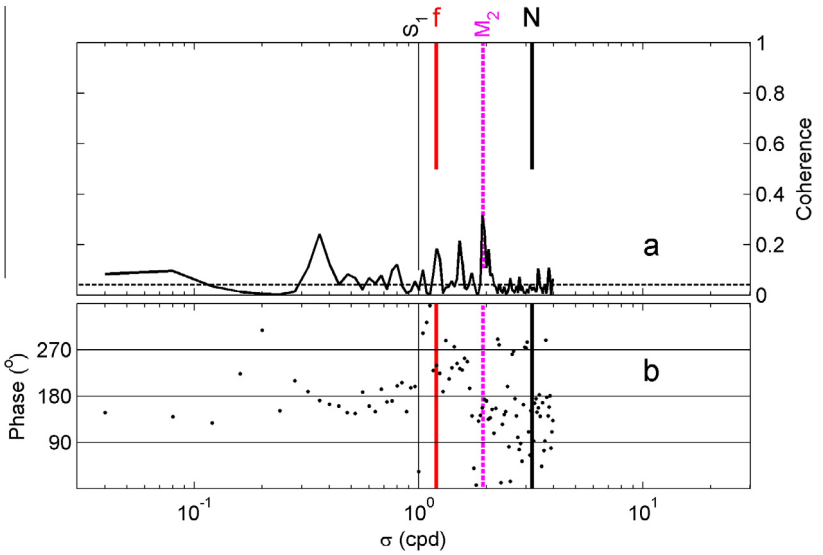

Fig. 8. As Fig. 6, but between PCR at sensors Py-a and Py-b.

1. PMT count rate (PCR)-spectra resemble those of kinetic energy, whilst those of Py-a also show relatively large tidal peaks partially resemble those in hydrostatic surface pressure data.
2. The correspondence between PCR and horizontal current components is weak, but significant at near-inertial, sub-inertial mesoscale and (for Py-a mainly) at tidal frequencies.
3. Corresponding phase differences between east-current components and PCR are about 180° for sub-inertial mesoscale motions and about 0°(360°) for near-inertial motions. The causes for optical variations are thus dependent on current magnitude and direction.
4. Near Pylos, the small surface tide and tidal current (=surface gradient) show significant coherence with PCR, but at opposite phases for the two sensors. This effect is attributed to impact caused by bioluminescent organisms that have different response as a function of current direction in the opposing PMTs.

Due to limited battery-life only low-sampling-rates could be obtained with the present stand-alone instrumentation. Future connections to shore should provide more detailed optical data using optical modules with 31 3″-diameter PMTs.

Acknowledgments

We thank the crews of R/V Pelagia and R/V Meteor for deployment and recovery of the moorings, respectively. We acknowledge the Netherlands Organisation for the Advancement of Scientific Research, NWO for support.

References

[1] I.G. Priede et al., Deep-Sea Res. I 55 (2008) 1474.
[2] G. Riccobene et al., Astropart. Phys. 1 (2007) 1.
[3] E.G. Anassontzis et al., Astropart. Phys. 34 (2010) 187.
[4] J. Craig et al., Deep-Sea Res. I 57 (2010) 1474.
[5] J.A. Aguilar et al., On behalf of the ANTARES collaboration, Astropart. Phys. 26 (2006) 314.
[6] KM3NeT, KM3NeT Technical Design Report for a deep-sea research infrastructure incorporating a very large volume neutrino telescope. ISBN 978-90-6488-033-9 (2011) Available from: <http://www.km3net.org/TDR/TDRKM3NeT.pdf>. For the latest information on the development of 3"-PMTs: see, Proceedings of 6th international workshop on very large volume neutrino telescopes: VLVvT 13, AIP Conf. Proc. 1630 (2014).
[7] O. Kavatsyuk, Q. Dorosti-Hasankiadeh, H. Löhner, Nucl. Instrum. Methods Phys. Res. A626–627 (2011) S154.
[8] P. Kooijman et al., Nucl. Instrum. Methods Phys. Res. A626–627 (2011) S139.
[9] S. Adrián-Martínez et al., The KM3NeT collaboration, Eur. Phys. J. C 74 (2014) 3056.
[10] H. van Haren, L. Gostiaux, Geophys. Res. Lett. 38 (2011) L22603, http://dx.doi.org/10.1029/2011GL049707.
[11] H. van Haren, Ocean Dyn. 54 (2004) 49.
[12] H. van Haren, C. Millot, Geophys. Res. Lett. 32 (2005) L24614, http://dx.doi.org/10.1029/2005GL023915.
[13] P.H. LeBlond, L.A. Mysak, Waves in the Ocean, Elsevier, Amsterdam, 1978. 602 pp.